

Structural Insights into the Substrate Recognition Mechanism of *Arabidopsis* GPP-Bound NUDX1 for Noncanonical Monoterpene Biosynthesis

Dear Editor,

In plants, monoterpenes are a large family of volatiles that play essential roles in communicating with the surrounding environment, including pollinator attraction, pathogen defense, and plant–plant interactions (Sun et al., 2016). Dozens of monoterpene derivatives have been widely applied in the pharmaceutical, nutraceutical, flavor, and fragrance industries. Because of their high economic value, the biosynthesis of monoterpenes has been thoroughly studied (Degenhardt et al., 2009; Vranova et al., 2013). Typically, such biosynthesis reactions are accomplished by various monoterpene synthases, which convert the 10-carbon prenyl diphosphate (usually geranyl pyrophosphate [GPP]) into a large range of products (Tholl and Gershenzon, 2015). A common carbocationic reaction mechanism for all monoterpene synthases starts with the ionization of GPP through removal of the pyrophosphate group, resulting in a carbocation intermediate that can undergo cyclization, hydride shifts, or other rearrangements (Degenhardt et al., 2009).

A monoterpene synthase-independent pathway was recently identified in *Rosa hybrid cultivar* (Magnard et al., 2015). One cytosolic hydrolase, *Rosa hybrid cultivar* Nudix1 (RhNUDX1), which belongs to the Nudix hydrolase family, catalyzes the transformation of GPP into geranyl monophosphate (GP) by hydrolyzing a single phosphate (Magnard et al., 2015; Sun et al., 2016) (Figure 1A). Notably, RhNUDX1 was discovered to be responsible for the production of geraniol in rose flowers. Hence, it has application potentials in the chemical or floral industry (Wurtzel and Kutchan, 2016). However, the underlying mechanism by which RhNUDX1 recognizes GPP is still unknown.

To answer these questions, we first sought to determine the complex structure of RhNUDX1 with geranyl compounds but were unsuccessful. Thus, we screened RhNUDX1 homologs from certain economically important crops and plants commonly used in research, such as *Arabidopsis thaliana*. These homologs from the Nudix family shared a conserved 23-amino acid sequence termed the Nudix motif (GX₅EX₇REUXEEXGU, where U is an aliphatic, hydrophobic residue), which is required for substrate catalysis (McLennan, 2006; Kraszewska, 2008). Based on full-length sequence searches, we selected eight protein candidates for further biochemical and structural studies (Supplemental Figure 1A). First, we detected the enzyme activity using liquid chromatography–tandem mass spectrometry (LC–MS/MS). All the selected proteins exhibited GPP hydrolysis activity (Supplemental Figure 1B), as exemplified by *Arabidopsis thaliana* Nudix1 (AtNUDX1). AtNUDX1 was shown to efficiently hydrolyze GPP to GP, and the mutant E56A (one of

three essential E variants in the core of Nudix box) completely abolished this activity (Figure 1A). Therefore, we chose AtNUDX1 and the E56A variant for crystallization.

We ultimately crystallized AtNUDX1 without GPP in the space group P2₁2₁2₁, determined the structure by molecular replacement based on the available coordinates (MutT, PDB: 4KYX), and refined the structure at a resolution of 1.39 Å (Supplemental Table 1). Most of the amino acids were well assigned in the distinct electron density map, except for five N-terminal residues. Although the cyclic electron density near the Nudix motif was difficult to model (Supplemental Figure 2A), three divalent cations were accommodated by the catalytic center of the Nudix box (Supplemental Figure 2B). These divalent cations are usually magnesium or manganese cations (Mildvan et al., 2005). In one asymmetric unit, two protein molecules displaying an almost identical conformation, formed an antiparallel dimer with an interface area of approximately 950 Å² (Figure 1B). Structural analysis revealed that the interface is primarily mediated by a network of water-mediated hydrogen bonds. The dimer interface contains 11 residues from each protomer and contains three regions: from residues P8 to V10, F45 to E47, and L71 to H86. The protein retains a dimeric structure in the soluble state, which was confirmed by size-exclusion chromatography (SEC) and analytical ultracentrifugation (AUC) analyses (Supplemental Figure 3).

AtNUDX1 adopts a typical Nudix fold (Mildvan et al., 2005; McLennan, 2006). The structure contains four β strands (β1, β5, β6, and β7) with additional mixed β sheets (β2, β3, β4, and β8) sandwiched by the catalytic helix (α1) and an orthogonally orientated C-terminal helix (α2) (Figure 1B). This arrangement appears to form a pocket. The Nudix motif displays a loop-helix-loop structure near the N terminus that is adjacent to the pocket. Importantly, the Nudix motif is responsible for divalent ion coordination and acts as the catalytically active site in Nudix family proteins (McLennan, 2006; Kraszewska, 2008).

To elucidate the structural basis of GPP hydrolysis by AtNUDX1, we attempted to determine the complex structure of GPP-bound AtNUDX1. After the E56A variant was crystallized, the crystals were saturated with GPP and the complex structure determination was ultimately successful (Supplemental Table 1). After the assignment of most of the AtNUDX1 amino acids in the electron density map, the density corresponding to the GPP molecule was clearly visible. In one asymmetric unit, four protein

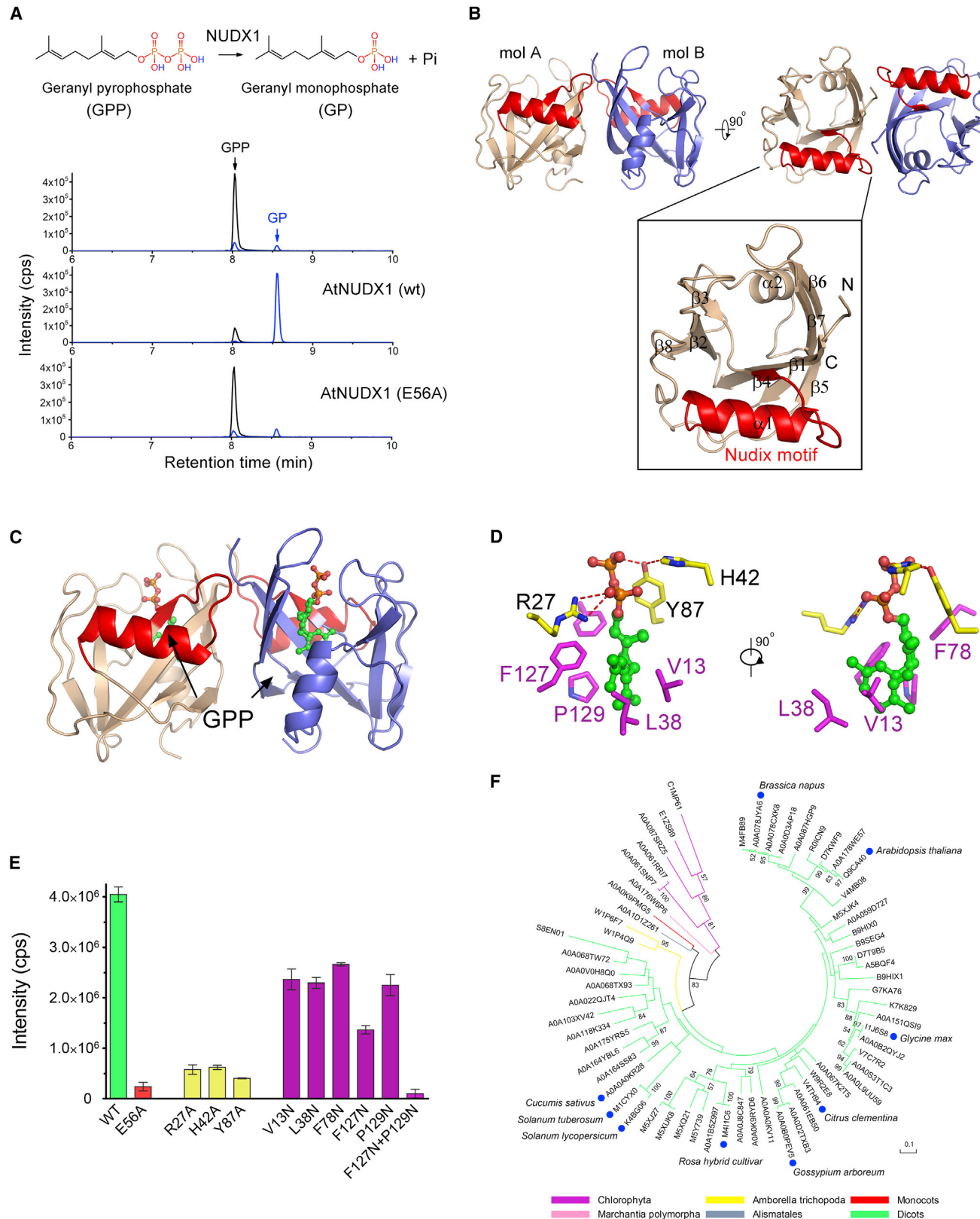


Figure 1. Structural Basis of GPP Hydrolysis by NUDX1.

(A) Schematic reaction of NUDX1 hydrolyzing GPP. NUDX1 cleaves the bond between the α -phosphate and the β -phosphate to generate GP and one phosphate (Pi). The LC-MS/MS chromatograms show the activity of AtNUDX1 and its variant E56A against GPP. Black traces indicate the ion intensities for the mass of GPP (m/z 313.10), and blue traces show the ion intensities for the mass of GP (m/z 233.10).

(legend continued on next page)

molecules bound four GPP substrates (each protein binds one GPP molecule) (Supplemental Figure 4A). The superposition of dimers in the GPP-free and GPP-bound state resulted in a root-mean-square deviation value of 0.44 Å over 137 C α atoms (Supplemental Figure 4B), implying that few conformational changes occurred upon GPP binding. The soluble GPP-bound AtNUDX1 complex remains in a dimer state based on our SEC and AUC data (Supplemental Figure 3D and 3E); therefore, the tetrameric complex is likely a consequence of crystal packing. To investigate the functional role of dimerization, we generated a series of mutations at the dimer interface to identify a monomer variant and analyze its hydrolase activity. After several unsuccessful trials, we eventually found that a mutation (V10K) can lead to the dissociation of the AtNUDX1 dimer. This monomeric variant showed efficient hydrolase activity comparable with the wild-type, suggesting that dimerization is dispensable for the catalytic function (Supplemental Figure 5).

In the substrate-bound structure, each subunit holds one GPP molecule in the core of the pocket (Figure 1C). GPP was coordinated by eight residues of AtNUDX1 via hydrogen bonds and hydrophobic interactions (Figure 1D). The oxygen atom on the α -phosphate was hydrogen bonded to the guanidinium group of R27, and the oxygen atom on the β -phosphate interacted with the side chains of H42 and Y87 through two hydrogen bonds (Figure 1D). The geranyl moiety of GPP was surrounded by a network of extensive hydrophobic contacts mediated by V13, L38, F78, F127, and P129. The importance of these residues was supported by the mutational analysis (Figure 1E). Indeed, the point mutation of the three residues participating in hydrogen-bond formation (R27A, H42A, and Y87A) largely caused the abolishment of the enzyme's GPP hydrolysis activity. The V13N, L38N, F78N, F127N, and P129N mutants retained approximately half of their catalyzing activity. Moreover, a double mutation (F127N and P129N) completely abrogated the enzyme activity, supporting the structural observations. These residues are highly conserved (Supplemental Figure 1A). Therefore, we introduced several point mutations back into RhNUDX1 for further validation. Consistent with the mutagenesis observations of AtNUDX1, four mutations in RhNUDX1 (R34A, L45N, Y94A, and F134N and P136N) led to severely compromised hydrolase activity toward GPP. Asparagine substitutions of V20, F85, and F134 decreased the enzyme activity by nearly half or more, whereas the two mutations (H49A and P136N) exhibited little effect on the catalytic reaction (Supplemental Figure 6). These results suggest that the proteins in the NUDX1 family may all be able to bind and act upon GPP.

Interestingly, the geranyl moiety of GPP displayed two conformations (Figure 1D). In the crystal, GPP can occur in two alternative states when bound to AtNUDX1. This phenomenon raises the possibility that AtNUDX1 can bind and subsequently hydrolyze similar skeletal molecules. To test our assumption, we used farnesyl pyrophosphate (FPP), a C15 sesquiterpene that contains one more isoprenyl unit than GPP in the terpene skeletal, to conduct a similar hydrolysis reaction. We identified the resulting compounds from the incubation of AtNUDX1 with FPP by LC-MS/MS. Similar to the GPP-to-GP reaction, FPP was converted to FP by cleaving the bond between α - and β -phosphate (Supplemental Figure 7A). Furthermore, the other eight homologs also showed activity toward FPP (Supplemental Figure 7B), including RhNUDX1, which is consistent with previous findings (Magnard et al., 2015). We also docked FPP in the pocket of AtNUDX1 and further minimized it by a molecular dynamics simulation (Supplemental Figure 7C). The final calculated interaction energy was estimated at -43.23 kcal/mol, thus indicating a stable interaction between the protein and FPP. However, the physiological role of this NUDX family capable of hydrolyzing FPP requires additional investigation.

To understand how this noncanonical monoterpene synthesis pathway is distributed and has evolved, we analyzed 486 homologous NUDX1 proteins from bacteria to eukaryotes (Supplemental Table 2). The phylogenetic tree revealed that the predominant majority of NUDX1 homologs can be clustered into four major groups: Proteobacteria (144 of 178); Dikarya (141 of 146), which contains two subgroups; dicots (53 of 63); and Vertebrata (63 of 75) (Supplemental Figure 8). Interestingly, most plant proteins form an evolutionarily conserved clade in dicots (Figure 1F), whereas only one protein from *Zostera marina* belongs to the monocots. This finding suggests that NUDX1 genes are divergently distributed in dicots and monocots and eventually evolved in dicots. The enzymatic assays demonstrated that the other seven homologous proteins from the clade also displayed catalytic activity toward these two substrates (Supplemental Figures 1B and 7B), implying the widespread occurrence of this noncanonical pathway. In the future, the genes involved in this unique monoterpene biosynthesis pathway will serve as an important foundation for understanding their roles in plant evolution.

The chemical compound industry has expressed increasing interest in enzymes, and investigations of enzymes for both natural and industrial usage are important and valuable for the synthesis of economically important compounds (Koksal et al., 2011). Notably, RhNUDX1, the key player in a unique monoterpene

(B) Overview of the dimeric structure of AtNUDX1 (molecule A in brown and molecule B in blue), and the Nudix motif is highlighted in red. The secondary structure elements and the N and C termini are labeled. All figures representing the structure were prepared with PyMOL (Schrödinger, LLC).

(C) Side view of the AtNUDX1 dimer ribbon representation with GPP coordination. GPP is illustrated using a green (geranyl moiety) and orange (diphosphate group) ball-and-stick representation.

(D) Close-up representation of the coordination of GPP by the side chains of the residues from the AtNUDX1 pocket. The residues involved in hydrogen-bond formation are shown as yellow sticks, and the hydrophobic residues are shown as magenta sticks.

(E) Catalytic activity of the mutations of the residues coordinating GPP. The activity was quantified by LC-MS/MS. Error bars represent the SEM of the ion intensity difference determined by three independent measurements.

(F) Maximum likelihood phylogenetic tree of NUDX1 homologs in the plant kingdom. For clarity, values of bootstrapping 1000 replicates below 50% are not shown. The UniProt accession numbers are depicted at each branch. The blue solid circles indicate the homologs applied in biochemical and structural studies.

Molecular Plant

Letter to the Editor

synthesis pathway, removes only one phosphate from the precursor GPP. This enzyme was reported to be much more efficient than known monoterpene synthases (Tholl and Gershenzon, 2015), indicating that it has application potential as a tool enzyme. Our investigations of the reaction of this enzyme showed that it not only differed from those of all known monoterpene synthases, which remove two phosphates in one reaction, but it also differed from classic nucleoside-diphosphate-hydrolysis (GPP does not contain the nucleoside moiety). These findings suggest an important role of this enzyme in evolution and functional divergence. Here, we provide the first structural views of GPP-free and GPP-bound AtNUDX1, the closest homolog of RhNUDX1 (Magnard et al., 2015). These structures imply that the pocket of AtNUDX1 contains several conserved hydrophobic residues and is responsible for accommodating the dynamic C10 hydrocarbon of GPP and possibly other similar molecules, such as FPP. Furthermore, our findings provide new opportunities for structure-guided enzyme engineering (Wurtzel and Kutchan, 2016) and the realization of new biosynthetic pathways for the industrially optimal biosynthetic production of fragrant monoterpenes.

ACCESSION NUMBERS

The atomic coordinates and structural factors of the three structures have been deposited in the Protein Data Bank (PDB) under accession codes PDB: 5WWD (GPP-free, wild-type protein), 5WY6 (apo E56A), and 5GP0 (GPP-bound complex).

SUPPLEMENTAL INFORMATION

Supplemental Information is available at *Molecular Plant Online*.

FUNDING

This work was supported by funds from the Ministry of Science and Technology (grant number 2015CB910900), the Fok Ying Tong Education Foundation (grant number 151021), the open funds of the National Key Laboratory of Crop Genetic Improvement, the Fundamental Research Funds for the Central Universities (program no. 2016BC018), and the Huazhong Agricultural University Scientific & Technological Self-Innovation Foundation (program no. 2013RC013).

AUTHOR CONTRIBUTIONS

Conceptualization, J.L., T.Z., and P.Y.; Methodology, J.L. and P.Y.; Software, Z.G., J.L., and H.L.; Formal Analysis, J.L., L.Q., and D.Z.; Investigation, J.L.; Writing – Original Draft, J.L., T.Z., and P.Y.; Writing – Review & Editing, J.L. and P.Y.; Supervision, T.Z. and P.Y.

ACKNOWLEDGMENTS

We would like to thank J. He at the Shanghai Synchrotron Radiation Facility (SSRF) beamline BL17U and R. Zhang at the SSRF beamline BL19U for

their on-site assistance. We would also like to thank the research associates F. Zhang and H. Sun at the Center for Protein Research (CPR) for their technical support and Dr. Z. Gong (Wuhan Institute of Physics and Mathematics) for performing the modeling. No conflict of interest declared.

Received: March 29, 2017

Revised: October 17, 2017

Accepted: October 18, 2017

Published: October 20, 2017

Jian Liu, Zeyuan Guan, Hongbo Liu,
Liangbo Qi, Delin Zhang, Tingting Zou and
Ping Yin*

National Key Laboratory of Crop Genetic Improvement and National Centre of Plant Gene Research, Huazhong Agricultural University, Wuhan 430070, China

*Correspondence: Ping Yin (yinping@mail.hzau.edu.cn)

<https://doi.org/10.1016/j.molp.2017.10.006>

REFERENCES

- Degenhardt, J., Kollner, T.G., and Gershenzon, J. (2009). Monoterpene and sesquiterpene synthases and the origin of terpene skeletal diversity in plants. *Phytochemistry* **70**:1621–1637.
- Koksal, M., Jin, Y., Coates, R.M., Croteau, R., and Christianson, D.W. (2011). Taxadiene synthase structure and evolution of modular architecture in terpene biosynthesis. *Nature* **469**:116–120.
- Kraszewska, E. (2008). The plant Nudix hydrolase family. *Acta Biochim. Pol.* **55**:663–671.
- Magnard, J.L., Rocca, A., Caissard, J.C., Vergne, P., Sun, P., Hecquet, R., Dubois, A., Hibrand-Saint Oyant, L., Jullien, F., Nicole, F., et al. (2015). PLANT VOLATILES. Biosynthesis of monoterpene scent compounds in roses. *Science* **349**:81–83.
- McLennan, A.G. (2006). The Nudix hydrolase superfamily. *Cell. Mol. Life Sci.* **63**:123–143.
- Mildvan, A.S., Xia, Z., Azurmendi, H.F., Saraswat, V., Legler, P.M., Massiah, M.A., Gabelli, S.B., Bianchet, M.A., Kang, L.W., and Amzel, L.M. (2005). Structures and mechanisms of Nudix hydrolases. *Arch. Biochem. Biophys.* **433**:129–143.
- Sun, P., Schuurink, R.C., Caissard, J.C., Huguene, P., and Baudino, S. (2016). My way: noncanonical biosynthesis pathways for plant volatiles. *Trends Plant Sci.* **21**:884–894.
- Tholl, D., and Gershenzon, J. (2015). BIOCHEMISTRY. The flowering of a new scent pathway in rose. *Science* **349**:28–29.
- Vranova, E., Coman, D., and Grisse, W. (2013). Network analysis of the MVA and MEP pathways for isoprenoid synthesis. *Annu. Rev. Plant Biol.* **64**:665–700.
- Wurtzel, E.T., and Kutchan, T.M. (2016). Plant metabolism, the diverse chemistry set of the future. *Science* **353**:1232–1236.